MCT1-Mediated Transport of L-Lactic Acid at the Inner Blood–Retinal Barrier: A Possible Route for Delivery of Monocarboxylic Acid Drugs to the Retina

Ken-ichi Hosoya[1,4], Tetsu Kondo[2], Masatoshi Tomi[1,4], Hitomi Takanaga[2,3,4], Sumio Ohtsuki[2,3,4], and Tetsuya Terasaki[2,3,4,5]

Received June 13, 2001; accepted September 9, 2001

Purpose. The aim of this study was to characterize L-lactic acid transport using a conditionally immortalized rat retinal capillary endothelial cell line (TR-iBRB2) as a model of *in vitro* inner blood–retinal barrier (iBRB) to obtain a better understanding of the transport mechanism at the iBRB.

Methods. TR-iBRB2 cells were cultured at 33°C, and L-lactic acid uptake was monitored by measuring [^{14}C]L-lactic acid at 37°C. The expression and mRNA level of monocarboxylate transporter (MCT)1 and MCT2 were determined by reverse transcription polymerase chain reaction (RT-PCR) and quantitative real-time RT-PCR with specific primers, respectively.

Results. The [^{14}C]L-lactic acid uptake by TR-iBRB2 cells increased up to a pH of 5.0 and was inhibited in the presence of 10 mM L-lactic acid. The [^{14}C]L-lactic acid uptake at pH 6.0 was both temperature- and concentration-dependent with a Michaelis–Menten constant of 1.7 mM and a maximum uptake rate of 15 nmol/(30 s · mg of protein). This process was reduced by carbonylcyanide *p*-trifluoromethoxyphenylhydrazone (protonophore), α-cyano-4-hydroxycinnamate, and *p*-chloromercuribenzenesulfonate (typical inhibitors for H^+-coupled monocarboxylic acid transport), suggesting that L-lactic acid uptake by TR-iBRB2 cells is a carrier-mediated transport process coupled with an H^+ gradient. [^{14}C]L-Lactic acid uptake was markedly inhibited by monocarboxylic acids but not dicarboxylic acids and amino acids. Moreover, salicylic and valproic acids competitively inhibited this process with an inhibition constant of 4.7 mM and 5.4 mM, respectively. Although MCT1 and MCT2 mRNA were found to be expressed in TR-iBRB2 cells, MCT1 mRNA was found to be present at a concentration 33-fold greater than that of MCT2 mRNA using quantitative real-time PCR. [^{14}C]L-Lactic acid was significantly reduced by 5-(*N,N*-hexamethylene)-amiloride at pH 7.4 and Na^+/H^+ exchanger 1 mRNA was expressed in TR-iBRB2 cells.

Conclusion. L-Lactic acid transport at the iBRB is an H^+-coupled and carrier-mediated mechanism via MCT1 that is competitively inhibited by monocarboxylate drugs.

KEY WORDS: MCT1; L-lactic acid transport; inner blood–retinal barrier; retinal capillary endothelial cell line.

[1] Faculty of Pharmaceutical Sciences, Toyama Medical and Pharmaceutical University, 2630, Sugitani, Toyama 930-0194, Japan.
[2] Department of Molecular Biopharmacy and Genetics, Graduate School of Pharmaceutical Sciences, Tohoku University, Aoba, Aramaki, Aoba-ku, Sendai 980-8578, Japan.
[3] New Industry Creation Hatchery Center, Tohoku University, Aoba, Aramaki, Aoba-ku, Sendai 980-8579, Japan.
[4] CREST of Japan Science and Technology Corporation (JST).
[5] To whom correspondence should be addressed. (e-mail: terasaki@mail.pharm.tohoku.ac.jp)

INTRODUCTION

Monocarboxylic acid transporters play an important role in the influx and efflux transport of monocarboxylate compounds, such as L-lactic acid, acetic acid, propionic acid, pyruvic acid, and ketone bodies (acetoacetic acid and β-hydroxybutyric acid) in the eye. H^+-coupled and Na^+-coupled L-lactic acid transport processes appear to be present in the corneal epithelium (1), endothelium (2), conjunctival epithelium (3), and retinal pigment epithelium (RPE) (4). From a physiological point of view, they may be involved in the efflux of excess L-lactic acid from corneal and retinal parenchymal cells. However, it is also an attractive route for monocarboxylate drug delivery to the posterior segment of the eye (5). Indeed, monocarboxylate drugs, such as salicylic acid, benzoic acid, and pravastatin, have been shown to be transported by H^+-coupled carrier-mediated transport processes in the intestine (6) and Caco-2 cells (7).

The retina produces aerobically more L-lactic acid than any other organ in the body (8), and L-lactic acid is produced even under anaerobic conditions (9). Moreover, L-lactic acid appears to be required as an energy source, in addition to D-glucose, in photoreceptors (9). To maintain full retinal function, the blood–retinal barrier (BRB) may regulate L-lactic acid movement between the circulating blood and the neural retina because the outer BRB (oBRB), i.e., RPE, expresses monocarboxylate transporter (MCT)1 on the apical side and MCT3 on the basal side (4). These may be involved in the efflux of L-lactic acid from the neural retina (4). On the other hand, retinal uptake index studies have provided evidence of saturable and pH-dependent L-lactic acid uptake from the circulating blood to the retina, suggesting L-lactic acid influx transport via MCT (10). However, this method cannot distinguish between retinal drug uptake by the inner BRB (iBRB) or oBRB routes. The iBRB, which is formed by complex tight junctions of retinal capillary endothelial cells (11), may play a key role in the influx and efflux transport on the vitreous side of the retina. Recently, Gerhart *et al.* (12) used immunohistochemical analysis to show that MCT1 is expressed at the iBRB, although our knowledge of the transport mechanism for L-lactic acid at the iBRB is still incomplete.

We recently established conditionally immortalized rat retinal capillary endothelial cell lines (TR-iBRB) from a transgenic rat harboring temperature-sensitive SV 40 large T-antigen gene. TR-iBRB cells express D-glucose transporter (GLUT1), efflux transporter (P-glycoprotein), and have endothelial markers (13), which suggests that they possess at least *in vivo* transport functions and are a suitable *in vitro* model for the iBRB (14). The purpose of the present study was to investigate the transport mechanism of L-lactic acid at the iBRB using TR-iBRB2 cells as an *in vitro* iBRB model.

MATERIALS AND METHODS

Animals

Male Wistar rats weighing 250 g to 300 g were purchased from Charles River Laboratories (Yokohama, Japan) and used as positive controls for reverse transcription polymerase chain reaction (RT-PCR). The investigations using rats described in this report conformed to the guidelines of the Ani-

0724-8741/01/1200-1669/0 © 2001 Plenum Publishing Corporation

mal Care Committee, Graduate School of Pharmaceutical Sciences, Tohoku University, and the ARVO Statement on the Use of Animals in Ophthalmic and Vision Research.

Materials

L-[U-^{14}C]Lactic acid sodium salt (154 mCi/mmol) was purchased from Amersham Life Science (Buckinghamshire, UK); endothelial cell growth factor (bovine) was obtained from Roche Diagnostics (Mannheim, Germany); fetal bovine serum from Moregate (Bulimba, Australia); benzylpenicillin potassium and streptomycin sulfate from Wako Pure Chemical Industries (Osaka, Japan); sodium bicarbonate-free Dulbecco's modified Eagle's medium powder (DMEM powder) from Nissui (Tokyo, Japan); and trypsin–EDTA from Gibco BRL (Grand Island, NY). All other chemicals were of reagent grade and available commercially.

RT-PCR Analysis

Total RNA was prepared from cells or rat tissues after washing with phosphate-buffered saline (PBS) using Trizol reagent (Gibco BRL). Tissues used as a control were isolated and then dipped in liquid nitrogen. Frozen samples were broken up using a hammer and immersed in Trizol reagent. Single-strand cDNA was made from 1 μg total RNA by reverse transcription (RT) using an oligo dT primer. PCR was performed using GeneAmp (PCR system 9700, Perkin–Elmer, Norwalk, CT) with MCT1-, MCT2-, and Na^+/H^+ exchanger 1 (NHE1)-specific primers through 30–35 cycles of 94°C for 30 s, 55°C for 1 min, and 72°C for 1 min. The sequences of the specific primers were as follows: the sense sequence was 5′-GAA AAA CTC AAG TCC AAA GAG TCT-3′ and the antisense sequence was 5′-AGA AGC CCA AGA AGA CAA TGA AA-3′ for rat MCT1: the sense sequence was 5′-CCT CTG CCC CCT AGC CCA TT-3′ and the antisense sequence was 5′-AAT ACA CAC AAT CCT CCC TCA GA-3′ for rat MCT2: the sense sequence was 5′-TAT GAG TAT GTG GGC ATC TCG G-3′ and the antisense sequence was 5′-GGC TCC CAC CAG TGG AAC TG-3′ for rat NHE1. The PCR products were separated by electrophoresis on agarose gel in the presence of ethidium bromide and visualized using an imager (EPIPRO 7000, Aisin, Aichi, Japan). PCR products of the expected length were then cloned into a plasmid vector using the p-GEM-T Easy Vector System I (Promega, Madison, WI). Several clones were then sequenced in both directions using a DNA sequencer (model 4200, LI-COR, Lincoln, NE).

Quantitative Real-Time PCR

The total RNA (1 μg/μL) was prepared from PBS-washed cells from each culture plate using Trizol reagent (Gibco BRL). Quantitative real-time PCR was performed using an ABI PRISM 7700 sequence detector system (PE Applied Biosystems, Foster City, CA) with 2X SYBR Green PCR Master Mix (PE Applied Biosystems) as per the manufacturer's protocol. To quantitate the amount of specific mRNA in the samples, a standard curve was generated for each run using the plasmid (pGEM-T Easy Vector System I, Promega) containing the gene of interest (dilution ranging from 0.1 fg/μL to 1 ng/μL). This enabled standardization of the initial RNA content of TR-iBRB2 cells relative to the amount of glyceraldehyde-3-phosphate dehydrogenase (GAPDH).

PCR was performed using MCT1-, MCT2-, or GAPDH-specific primers through 40 cycles of 95°C for 30 s, 60°C for 1 min, and 72°C for 1 min after pre-incubation at 95°C for 10 min. The specific primers for MCT1 and MCT2 are those listed above and for GAPDH as follows: the sense sequence was 5′-TGA TGA CAT CAA GAA GGT GGT GAA G-3′ and the antisense sequence was 5′-TCC TTG GAG GCC ATG TAG GCC AT-3′.

Cell Culture and Uptake Experiments

TR-iBRB2 cells were grown routinely in collagen type I-coated tissue culture flasks (Becton Dickinson, Bedford, MA) at 33°C under 5% CO_2/air. The permissive temperature for TR-iBRB cells in culture is 33°C due to the expression of temperature-sensitive large T-antigens (13). The culture medium consisted of DMEM supplemented with 20 mM sodium bicarbonate, 15 μg/mL endothelial cell growth factor, 100 U/mL benzylpenicillin potassium, 100 μg/mL streptomycin sulfate, and 10% fetal bovine serum according to a previous report (13).

For the uptake study, cells having passage times between 60 and 80 were used. TR-iBRB2 cells (1×10^5 cells/cm^2) were cultured at 33°C for 2 days on rat tail collagen type I-coated 24-well plates (Becton Dickinson). After removal of culture medium, cells were washed with ECF-HEPES buffer (122 mM NaCl; 3 mM KCl; 0.4 mM K_2HPO_4; 25 mM $NaHCO_3$; 1.4 mM $CaCl_2$; 1.4 mM $MgSO_4 \cdot 7H_2O$; 10 mM HEPES, pH 7.4; 290 ± 15 mOsm/kg). Uptake was initiated by applying 200 μL ECF-MEM buffer (117 mM NaCl; 3 mM KCl; 0.4 mM K_2HPO_4; 25 mM $NaHCO_3$; 1.4 mM $CaCl_2$; 1.4 mM $MgSO_4 \cdot 7H_2O$; 20 mM MES, pH 5.0 to 6.5; 290 ± 15 mOsm/kg) or 200 μL ECF-HEPES buffer (pH 7.0 to 7.4) containing [^{14}C]L-lactic acid (0.4 μCi/well). The uptake study was performed at 37°C due to the physiological temperature. After a predetermined time period, uptake was terminated by suctioning off the applied solution and immersing the plates in ice-cold ECF-HEPES buffer (pH 7.4). The cells were then solubilized in 1 mL of 1% Triton X-100/PBS. Fifteen microliters of the solution was taken for protein assay by the DC protein assay kit (Bio–Rad, Hercules, CA) using bovine serum albumin as a standard. The remainder of the sample (500 μL) was mixed with 5 mL of scintillation cocktail (Hionic-fluor, Packard, Meriden, CT) to measure the radioactivity in a liquid scintillation counter (LS 6500, Beckman, Fullerton, CA). The uptake was expressed as the cell-to-medium concentration calculated as follows:

$$\text{Cell–to–medium concentration ratio (C/M ratio, μL/mg protein)} = \frac{[^{14}\text{C}]\text{L–Lactinc acid concentration in the cell (dpm/mg protein)}}{[^{14}\text{C}]\text{L–Lactic acid concentration in the medium (dpm/μL)}}$$

The [^{14}C]inulin (NEN Life Science Products, Boston, MA) uptake study was performed to estimate the volume of adhering water. The resulting C/M ratio was 0.1~0.2 μL/mg protein and 10-fold less than the C/M ratio of [^{14}C]L-lactic acid. Therefore, adhering water was ignored when calculating the C/M ratio.

Data Analysis

For kinetic studies, the Michaelis–Menten constant (K_m) and the maximum uptake rate (V_{max}) of [^{14}C]L-lactic acid were estimated from the following equation using the nonlinear least-square regression analysis program, MULTI (15).

$$V = \frac{V_{max} \cdot S}{K_m + S} + P_{non} \cdot S$$

where V, S, and P_{non} are the uptake rate of L-lactic acid at 30 s, the concentration of L-lactic acid, and the non-saturable uptake clearance, respectively. The inhibition constant (K_i) was estimated in the presence of monocarboxylates from the following equation using MULTI (15),

$$V = \frac{V_{max} \cdot S}{K_m \cdot \left(1 + \frac{I}{K_i}\right) + S} + P_{non} \cdot S$$

where I is the concentration of inhibitor.

Unless otherwise indicated, all data represent the mean ± standard error of the mean. An unpaired, two-tailed Student's *t* test was used to determine the significance of differences between two group means. Statistical significance among means of more than two groups was determined by one-way analysis of variance (ANOVA) followed by the modified Fisher's least squares difference method.

RESULTS

The pH Dependence of [^{14}C]L-Lactic Acid Uptake

The effect of the uptake medium pH on [^{14}C]L-lactic acid uptake by TR-iBRB2 cells was examined over the pH range 5.0 to 7.4 (Fig. 1A). The [^{14}C]L-lactic acid uptake at 30 s markedly increased after acidification in the absence of unlabeled L-lactic acid. The [^{14}C]L-lactic acid uptake at pH 6.0 and 5.0 was 2.4- and 3.0-fold greater, respectively, than that at pH 7.4. However, in the presence of 10 mM unlabeled L-lactic acid, the [^{14}C]L-lactic acid uptake at pH 5.0, 6.0, and 7.4 was significantly inhibited by 65.7%, 44.6%, and 23.9%, respectively, supporting the suggestion that [^{14}C]L-lactic acid uptake by TR-iBRB2 cells involves pH-dependent uptake. The following uptake experiments were performed at pH 6.0 to characterize the L-lactic acid transport mechanism because this gives a higher uptake than that at pH 7.4 and is closer to the physiological pH than pH 5.0 (16).

Time–Course of [^{14}C]L-Lactic Acid Uptake at pH 6.0

The time–courses of [^{14}C]L-lactic acid uptake at pH 6.0 and 37°C or 4°C, are shown in Figure 1B. The [^{14}C]L-lactic acid uptake was linear for at least 180 s. At 4°C, the uptake rate was reduced by more than 80% over 180 s, supporting the belief that [^{14}C]L-lactic acid uptake is a temperature-dependent process.

Concentration Dependence of [^{14}C]L-Lactic Acid Uptake at pH 6.0

Figure 2 shows the concentration-dependent uptake of [^{14}C]L-lactic acid by TR-iBRB2 cells. Performing an analysis using an Eadie–Scatchard plot, the intracellular L-lactic acid uptake was found to consist of saturable and non-saturable processes (Fig. 2, inset). Nonlinear least-square regression analysis revealed that the K_m, V_{max}, and P_{non} were 1.66 ± 0.47 mM, 15.1 ± 4.7 nmol/(30 s · mg of protein), and 2.77 ± 0.50 μL/(30 s · mg of protein), respectively (mean ± standard deviation).

Effect of Inhibitory Conditions on [^{14}C]L-Lactic Acid Uptake at pH 6.0

[^{14}C]L-Lactic acid uptake by TR-iBRB2 cells was examined to determine whether this intracellular uptake process

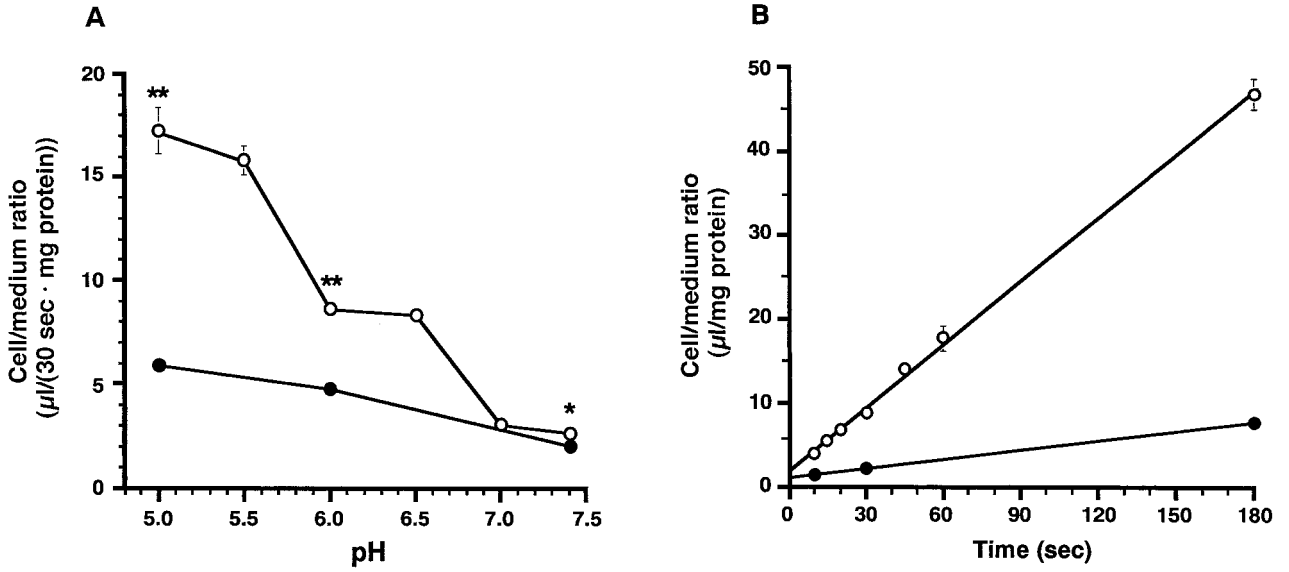

Fig. 1. The pH dependence of [^{14}C]L-lactic acid uptake by TR-iBRB2 cells (A) and time-courses of [^{14}C]L-lactic acid uptake by TR-iBRB2 cells (B). (A) The [^{14}C]L-lactic acid (13.0 μM) uptake at each pH was measured in the absence (○) or presence (•) of 10 mM L-lactic acid at 30 s and 37°C. Each point represents the mean ± standard error of the mean (n = 4). *$P < 0.05$, **$P < 0.001$, significantly different from the cell/medium ratio in the presence of 10 mM L-lactic acid. (B) The [^{14}C]L-lactic acid (13.0 μM) uptake was measured at pH 6.0 and 37°C (○) or 4°C (•). Each point represents the mean ± standard error of the mean (n = 3–4).

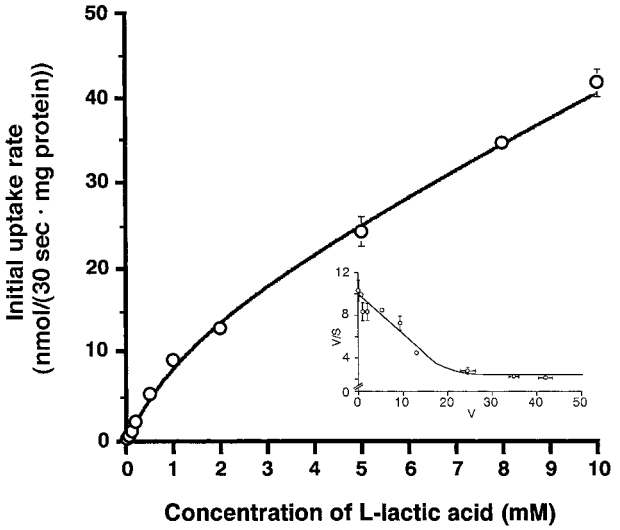

Fig. 2. Concentration dependence of L-lactic acid uptake by TR-iBRB2 cells. The [^{14}C]L-lactic acid (13.0 μM) uptake was measured at 37°C and pH 6.0. Each point represents the mean ± standard error of the mean (n = 3–4). Inset: Eadie–Scatchard plot exhibiting saturable and non-saturable uptake processes. The K_m is 1.66 ± 0.47 mM, V_{max} is 15.1 ± 4.7 nmol/(30 s · mg of protein), and P_{non} is 2.77 ± 0.50 μL/(30 s · mg of protein) (mean ± standard deviation).

requires metabolic energy and is driven by the inwardly directed H^+ gradient. The results are summarized in Table I. 2,4-Dinitrophenol at 10 mM and sodium azide at 10 mM significantly reduced the uptake of [^{14}C]L-lactic acid by 88.0% and 59.8%, respectively. In addition, carbonylcyanide *p*-trifluoromethoxyphenylhydrazone at 50 μM, α-cyano-4-hydroxycinnamic acid at 5 mM, and *p*-chloromercuribenzenesulfonic acid at 1 mM also significantly inhibited [^{14}C]L-lactic acid uptake by 44.4%, 87.3%, and 24.8%, respectively. However, replacement of Na^+ with choline or 0.1 mM 4,4′-diisothiocyanostilbene-2,2′-disulfonic acid had no effect on [^{14}C]L-lactic acid uptake.

Table I. Effect of Several Inhibitory Conditions on [^{14}C]L-Lactic Acid Uptake by TR-iBRB2 cells

Conditions	Relative uptake rate (% of control)
Control	100 ± 2
10 mM NaN_3	40.2 ± 3.2**
1 mM DNP (0.1% DMSO)[a]	12.0 ± 1.5**
0.1 mM DIDS	121 ± 6
Na^+-free condition	87.2 ± 2.2
50 μM FCCP (0.5% EtOH)[a]	55.6 ± 6.3**
5 mM 4-CHC	12.7 ± 1.2**
1 mM *p*CMBS	75.2 ± 2.5*

DNP, 2,4-Dinitrophenol; DIDS, 4,4′-diisothiocyanostilbene-2,2′-disulfonic acid; FCCP, carbonylcyanide *p*-trifluoromethoxyphenylhydrazone; 4-CHC, α-cyano-4-hydroxycinnamic acid; *p*CMBS, *p*-chloromercuribenzenesulfonic acid.

TR-iBRB2 cells were preincubated with DNP or NaN_3 for 5 min. The [^{14}C]L-lactic acid uptake was measured at 37°C and pH 6.0 for 30 s. Each value represents the mean ± standard error of the mean (n = 4–12).

* $P < 0.01$, ** $P < 0.001$, significantly different from control.

[a] Controls were performed in 0.1% DMSO solution or 0.5% ethanol solution.

Table II. Inhibitory Effect of Several Compounds on [^{14}C]L-Lactic Acid Uptake by TR-iBRB2 Cells

Inhibitors	Relative uptake rate (% of control)
Control	100 ± 2
L-Lactic acid	37.1 ± 1.4**
D-Lactic acid	57.5 ± 2.8**
Acetic acid	66.5 ± 4.4**
Pyruvic acid	23.3 ± 1.4**
Propionic acid	67.6 ± 2.2**
Valproic acid	33.4 ± 1.7**
Benzoic acid	34.1 ± 1.9**
Salicylic acid	33.6 ± 2.2**
Nicotinic acid	39.6 ± 1.6**
Glutaric acid	103.2 ± 2.5
Phthalic acid	76.8 ± 2.9*
p-Aminohippuric acid	89.7 ± 2.2
L-Glutamic acid	107 ± 6
L-Phenylalanine	120 ± 6
L-Arginine	102 ± 2

The [^{14}C]L-lactic acid uptake was measured at 37°C and pH 6.0 for 30 s in the presence of each 10 mM inhibitor.

Each value represents the mean ± standard error of the mean (n = 3–12).

* $P < 0.01$, ** $P < 0.001$, significantly different from control.

Inhibitory Effect of Several Compounds on [^{14}C]L-Lactic Acid Uptake at pH 6.0

The effect of monocarboxylic acids, amino acids, and other organic anions on [^{14}C]L-lactic acid uptake by TR-iBRB2 cells is summarized in Table II. L-Lactic acid, pyruvic

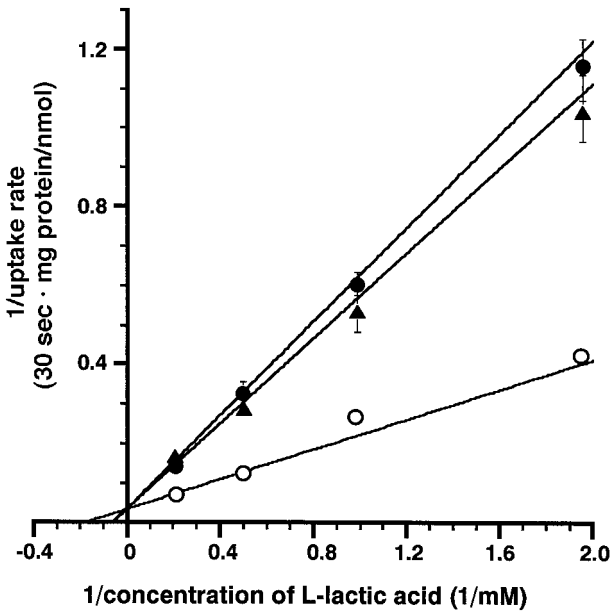

Fig. 3. Lineweaver–Burk plot of L-lactic acid uptake by TR-iBRB2 cells. The [^{14}C]L-lactic acid (13.0 μM) uptake was measured in the absence (○) and presence of 10 mM salicylic acid (•) or 10 mM valproic acid (▲) at 37°C and pH 6.0. Each point represents the mean ± standard error of the mean (n = 4).

acid, valproic acid, benzoic acid, salicylic acid, and nicotinic acid markedly inhibited [^{14}C]L-lactic acid uptake by up to 76.7%. D-Lactic acid, acetic acid, and propionic acid significantly inhibited this process by 42.5%, 33.5%, and 32.4%, respectively. In contrast, dicarboxylic acids, L-glutamic acid, L-phenylalanine, and L-arginine had no marked effect on [^{14}C]L-lactic acid uptake.

Mechanism of Inhibition by Monocarboxylic Acids

To identify the mechanism of inhibition by aromatic or aliphatic monocarboxylate drugs, we determined the uptake rate of [^{14}C]L-lactic acid by TR-iBRB2 cells in the presence of 10 mM salicylic acid or 10 mM valproic acid (Fig. 3). A Lineweaver–Burk plot for [^{14}C]L-lactic acid uptake in the presence of salicylic acid and valproic acid showed competitive inhibition of [^{14}C]L-lactic acid uptake by salicylic acid and valproic acid with a K_i value of 4.66 ± 0.16 and 5.38 ± 0.58 mM, respectively (mean ± standard deviation).

Expression of Monocarboxylic Acid Transporter mRNA in TR-iBRB2

Inhibition studies suggest that [^{14}C]L-lactic acid uptake by TR-iBRB2 cells is an H^+-coupled monocarboxylic acid uptake process. Therefore, RT-PCR experiments were performed to determine the expression of MCT1 and MCT2 in TR-iBRB2 cells using total RNA isolated from TR-iBRB2 cells, heart, and liver as a positive, control, respectively, and specific primers of rat MCT1 or rat MCT2 (Fig. 4, A and B). TR-iBRB2 cells expressed both MCT1 and MCT2 at 801 and 447 bp, respectively. The rat heart and liver were used as the corresponding positive control. The nucleotide sequence of the bands of TR-iBRB2 cells was virtually identical to rat MCT1, with a homology of 100% (17), and rat MCT2, with a homology of 99.5% (GeneBank accession number U62316). Quantitative real-time PCR showed that the MCT1 and MCT2 mRNA content relative to the amount of GAPDH mRNA (MCT1/GAPDH and MCT2/GAPDH) was $7.36 \times 10^{-2} \pm 0.32 \times 10^{-2}$ and $2.23 \times 10^{-3} \pm 0.18 \times 10^{-3}$, respectively (Fig. 4C). Accordingly, the expression of MCT1 mRNA was 33-fold greater than that of MCT2 mRNA in TR-iBRB2 cells.

Effect of Na^+/H^+ Exchanger on [^{14}C]L-Lactic Acid Uptake at pH 7.4

The inhibitory effect of 5-(*N,N*-hexamethylene)-amiloride (HMA), an Na^+/H^+ exchanger (NHE) inhibitor, on [^{14}C]L-lactic acid uptake was examined at physiological pH (pH 7.4) (Fig. 5A). The uptake was performed for 30 min in the presence of each concentration of HMA. [^{14}C]L-Lactic acid uptake by TR-iBRB2 cells was significantly reduced by 41.5%, 62.3%, and 61.2% by 1 μM, 50 μM, and 100 μM HMA, respectively. To investigate NHE mRNA expression in TR-iBRB2 cells, RT-PCR analysis was performed using total RNA isolated from TR-iBRB2 cells and rat intestine as a positive control specimen. When using specific primers of rat NHE1, NHE1 was expressed at 386 bp in TR-iBRB2 cells (Fig. 5B). The nucleotide sequence of the bands of TR-iBRB2 cells was virtually identical to rat NHE1, with a homology of 99.7% (18).

DISCUSSION

This study demonstrates that TR-iBRB2 cells that are used as an *in vitro* iBRB model produce L-lactic acid uptake

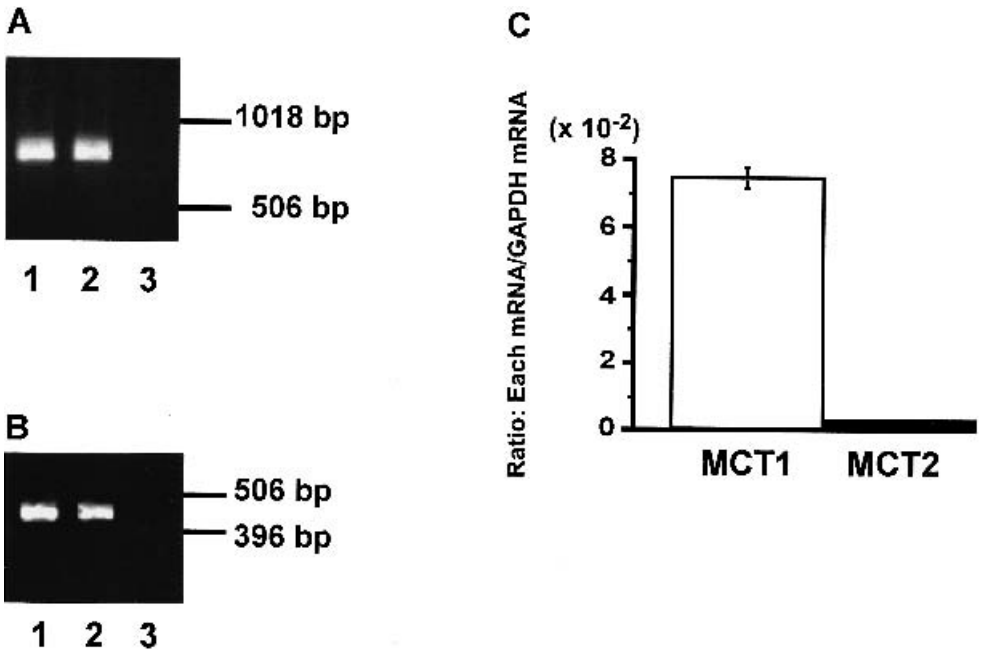

Fig. 4. Reverse transcription polymerase chain reaction analysis of rat MCT1 (A) and MCT2 (B), and the amount of MCT1 and MCT2 (C) in TR-iBRB2 cells. (A) Lane 1, heart as a positive control for MCT1; lane 2, TR-iBRB2 cells in the presence of reverse transcriptase; lane 3, TR-iBRB2 cells in the absence of reverse transcriptase. (B) Lane 1, liver as a positive control for MCT2; lane 2, TR-iBRB2 cells in the presence of reverse transcriptase; lane 3, TR-iBRB2 cells in the absence of reverse transcriptase. (C) Total RNA was prepared from each culture plate. The MCT1 and MCT2 mRNA content relative to the amount of GAPDH (MCT1/GAPDH and MCT2/GAPDH) was $7.36 \times 10^{-2} \pm 0.32 \times 10^{-2}$ and $2.23 \times 10^{-3} \pm 0.18 \times 10^{-3}$, respectively. Each value represents the mean ± standard error of the mean (n = 4). Accordingly, the ratio of MCT1 and MCT2 (MCT1/MCT2) was 33.0.

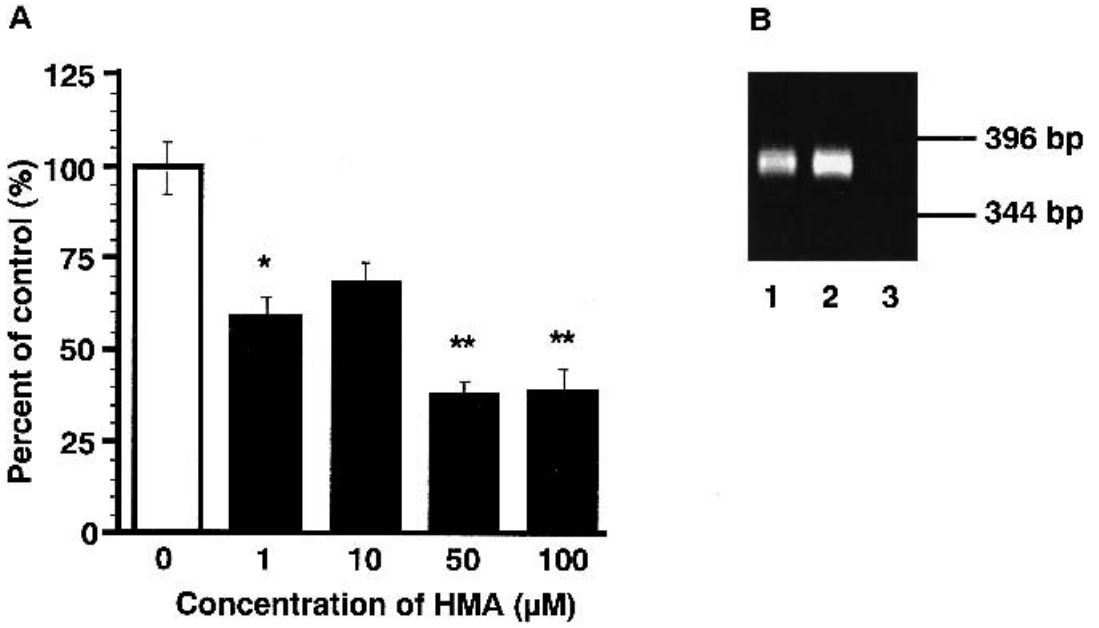

Fig. 5. Inhibitory effect of 5-(*N,N*-hexamethylene)-amiloride (HMA) on [^{14}C]L-lactic acid uptake by TR-iBRB2 cells (A) and reverse transcription polymerase chain reaction analysis of Na^+/H^+ exchanger 1 (NHE1) in TR-iBRB2 cells (B). (A) The [^{14}C]L-lactic acid (13.0 μM) uptake was measured in the absence or presence of HMA at pH 7.4 for 30 min. Each point represents the mean ± standard error of the mean (n = 4). $*P < 0.05$, $**P < 0.01$, significantly different from control (without HMA). (B) Lane 1, small intestine as a positive control; lane 2, TR-iBRB2 cells in the presence of reverse transcriptase; lane 3, TR-iBRB2 cells in the absence of reverse transcriptase.

via an H^+-coupled carrier-mediated transport process. This process takes place in a pH-, temperature-, and concentration-dependent manner (Figs. 1 and 2). The corresponding K_m and V_{max} values are 1.66 mM and 15.1 nmol/(30 s · mg of protein), respectively. This K_m value is identical to that of L-lactic acid transport (K_m = 1.8 mM) across the blood–brain barrier measured using the brain uptake index method (19) and is close to the L-lactic acid concentration in the circulating blood (1 mM) (20). The uptake clearance (CL) of L-lactic acid in TR-iBRB2 cells was estimated to be 9.10 μL/(30 s · mg of protein) according to $CL = V_{max}/K_m$. This is 3.3-fold greater than that of the non-saturable uptake clearance, 2.77 μL/(30 s · mg of protein). This suggests that L-lactic acid uptake in TR-iBRB2 cells is carrier mediated rather than taking place in accordance with the pH-partition theory (21). Indeed, at pH from 5.0 to 7.4, over 90% of the L-lactic acid is present in its ionized form in the medium because of the fact that the pK_a of L-lactic acid is 3.86 (22). Moreover, L-lactic acid uptake by TR-iBRB2 cells suggests an energy-dependent secondary active transport process due to inhibition by 2,4-dinitrophenol and sodium azide (Table I), which act as an uncoupler of oxidative phosphorylation and a respiratory chain inhibitor, respectively. The inhibition by carbonylcyanide *p*-trifluoromethoxyphenylhydrazone, a protonophore, and α-cyano-4-hydroxycinnamic acid and *p*-chloromercuribenzenesulfonic acid, both typical inhibitors of H^+-coupled monocarboxylic acid transport (23) (Table I), suggests that L-lactic acid uptake requires an inward H^+ gradient and involves an H^+-coupled monocarboxylic acid transporter. However, the absence of inhibition of [^{14}C]L-lactic acid uptake under Na^+-free conditions and in the presence of 4,4′-diisothiocyanostilbene-2,2′-disulfonic acid, an anion-exchange inhibitor (Table I), suggests no involvement of an Na^+-dependent L-lactic acid transporter and anion exchanger in L-lactic acid uptake. An H^+ gradient in TR-iBRB2 cells appears to be generated by NHE. NHE1 mRNA is expressed in TR-iBRB2 cells (Fig. 5B), and [^{14}C]L-lactic acid uptake is inhibited by a specific inhibitor of NHE at pH 7.4, i.e., HMA (24) (Fig. 5A).

The H^+-coupled L-lactic acid uptake by TR-iBRB2 cells appears to be specific for monocarboxylic acids. This is indicated by the 32% to 77% inhibition of [^{14}C]L-lactic acid uptake by monocarboxylic acids and by the absence of, or only slight, inhibition by dicarboxylic acids, amino acids, and a zwitterionic compound (Table II). The H^+-coupled L-lactic acid uptake by TR-iBRB2 cells appears to exhibit stereoselectivity for the L-isomer. The degree of inhibition by D-lactic acid of [^{14}C]L-lactic acid uptake by TR-iBRB2 cells is 20% less than that produced by L-lactic acid (Table II). Although both MCT1 and MCT2 mRNA were expressed in TR-iBRB2 cells, quantitative real-time PCR analysis supported that hypothesis that MCT1 mRNA is expressed predominantly in TR-iBRB2 cells (Fig. 4C). This result is consistent with the immunohistochemical results for iBRB reported by Gerhart *et al.* (12). Therefore, MCT1 most probably acts on L-lactic acid transport at the iBRB as well as at the blood–brain barrier (17).

Salicylic and valproic acids, which are model monocarboxylate drugs, competitively inhibited [^{14}C]L-lactic acid uptake with an apparent K_i value of 4.7 mM and 5.4 mM, respectively. Both values are comparable with the K_i of 20 mM and 3.9 mM for [^{14}C]benzoic acid uptake by Caco-2 cells in the presence of 10 mM salicylic acid and 10 mM valproic acid, respectively (7). Moreover, MCT1 is expressed in Caco-2 cells (25). L-Lactic acid uptake by TR-iBRB2 cells described in the current study most likely participates in the delivery of monocarboxylate drugs from the circulating blood to the retina. Alm and Törnquist (10), using the retinal uptake index

method, reported that L-lactic acid transport from the circulating blood to the retina occurred in a pH- and concentration-dependent manner, suggesting L-lactic acid influx transport via MCT although the contribution of the iBRB or oBRB route was unclear. From the drug delivery point of view, MCT1 at the iBRB may be a conduit for the entry of monocarboxylate drugs into the retina. If we wish to perform drug delivery to the retina, it is hard for drugs to reach the retina via the cornea and conjunctival route after the instillation of drops (5). Therefore, the iBRB, which expresses several transporters and transport systems, is a potential route for drug delivery to the retina from the circulating blood, as is the case with the blood–brain barrier (22). However, the polarization of TR-iBRB2 cells has not been established with functional and biochemical parameters.

One possible physiological role for MCT1 may be to promote the efflux L-lactic acid from the retina to the circulating blood under normal physiological conditions. This is because L-lactic acid is produced in the retina at a concentration of 7~13 mM (26), which is 10-fold greater than that in plasma (1 mM) (20). Therefore, it seems that the L-lactic acid concentration gradient operates from the retina to the circulating blood. Moreover, accumulation of L-lactic acid in the retina makes the pH more acidic and increases the osmolality (27), suggesting that the H^+ gradient operates from the retina to the blood. Philp *et al*. (4) reported that MCT1 and MCT3 are expressed on the apical and basal sides of the RPE, respectively. They suggested that these play a role in the efflux transport of L-lactic acid from the retina to the circulating blood across the RPE. Taken together, TR-iBRB2 cells predominantly express MCT1, which is involved in the uptake of H^+-coupled monocarboxylic acids. It may involve not only the influx transport of monocarboxylate drugs from the blood to the retina but also the efflux transport from the retina to the blood of excess of L-lactic acid to maintain homeostasis of the neural retina. Although it appears contradictory to argue that the secondary active transporter is involved in both influx and efflux transport at the iBRB, L-lactic acid transport across the blood–brain barrier also seems to be bidirectional (28,29). Further studies are needed to investigate the polarization of TR-iBRB2 cells. This approach will clarify the main contribution of MCT1 to influx or efflux transport at the iBRB. This information is important issue in regard to retinal monocarboxylate drug delivery via MCT1 at the iBRB.

In conclusion, L-lactic acid uptake at the iBRB is an H^+-coupled carrier-mediated transport process. The current results and previous reports support the idea that MCT1 is responsible for L-lactic acid transport at the iBRB (12). This is the first demonstration of the transport mechanism for L-lactic acid at the iBRB. These findings provide important information to help our understanding of the physiological role of the iBRB and drug delivery to the neural retina.

ACKNOWLEDGMENTS

We thank N. Funayama for secretarial assistance. This study was supported, in part, by a Grant-in-Aid for Scientific Research from the Ministry of Education, Science, Sports, and Culture, Japan. It was also support, in part, by The Nakatomi Foundation, The Suzuken Memorial Foundation, and The Mochida Memorial Foundation for Medical and Pharmaceutical Research.

REFERENCES

1. J. A. Bonanno. Lactate-proton cotransport in rabbit corneal epithelium. *Curr. Eye Res.* **9**:707–712. (1990).
2. C. Giasson and J. A. Bonanno. Facilitated transport of lactate by rabbit corneal endothelium. *Exp. Eye Res.* **59**:73–81 (1994).
3. Y. Horibe, K. Hosoya, K. Kim, and V. H. L. Lee. Carrier-mediated transport of monocarboxylate drugs in the pigmented rabbit conjunctiva. *Invest. Ophthalmol. Vis. Sci.* **39**:1436–1443 (1998).
4. N. J. Philp, H. Yoon, and E. F. Grollman. Monocarboxylate transporter MCT1 is located in the apical membrane and MCT3 in the basal membrane of rat RPE. *Am. J. Physiol.* **274**:R1824–R1828 (1998).
5. V. H. L. Lee and K. Hosoya. Drug delivery to the posterior segment. In S. J. Ryan (ed.), *Retina Third Edition,* Mosby, St. Louis, Missouri, 2001, pp. 2270–2285.
6. I. Tamai, H. Takanaga, H. Maeda, T. Ogthara, M. Yoneda, Y. Suzuki, and A. Tsuji. Proton-cotransport of pravastatin across intestinal brush-border membrane. *Pharm. Res.* **12**:1727–1732 (1995).
7. A. Tsuji, H. Takanaga, I. Tamai, and T. Terasaki. Transcellular transport of benzoic acid across Caco-2 cells by a pH-dependent and carrier-mediated transport mechanism. *Pharm. Res.* **11**:30–37 (1994).
8. C. N. Graymore. Biochemistry of retina. In C. N. Graymore (ed.), *Biochemistry of the Eye,* Academic Press, New York, 1970, pp. 645–735.
9. C. L. Poitry–Yamate, S. Poitry, and M. Tsacopoulos. Lactate released by Müller glial cells is metabolized by photoreceptors from mammalian retina. *J. Neurosci.* **15**:5179–5191 (1995).
10. A. Alm and P. Törnquist. Lactate transport through the blood–retinal and the blood-brain barrier in rats. *Ophthalmic Res.* **17**: 181–184 (1985).
11. P. A. Stewart and U. I. Tuor. Blood–eye barriers in the rat: correlation of ultrastructure with function. *J. Comp. Neurol.* **340**: 566–576 (1994).
12. D. Z. Gerhart, R. L. Leino, and L. R. Drewes. Distribution of monocarboxylate transporters MCT1 and MCT2 in rat retina. *Neuroscience* **92**:367–375 (1999).
13. K. Hosoya, M. Tomi, S. Ohtsuki, H. Takanaga, M. Ueda, N. Yanai, M. Obinata, and T. Terasaki. Conditionally immortalized retinal capillary endothelial cell lines (TR-iBRB) expressing differentiated endothelial cell functions derived from a transgenic rat. *Exp. Eye Res.* **72**:163–172 (2001).
14. T. Terasaki and K. Hosoya. Conditionally immortalized cell lines as a new in vitro model for the study of barrier functions. *Biol. Pharm. Bull.* **24**:111–118 (2001).
15. K. Yamaoka, Y. Tanigawara, T. Nakagawa, and T. Uno. A pharmacokinetic analysis program (MULTI) for microcomputer. *J. Pharmacobio-Dyn.* **4**:879–885 (1981).
16. Y. Kido, I. Tamai, M. Okamoto, F. Suzuki, and A. Tsuji. Functional clarification of MCT1-mediated transport of monocarboxylic acids at the blood–brain barrier using in vitro cultured cells and in vivo BUI studies. *Pharm. Res.* **17**:55–62 (2000).
17. H. Takanaga, I. Tamai, S. Inaba, Y. Sai, H. Higashida, H. Yamamoto, and A. Tsuji. cDNA cloning and functional characterization of rat intestinal monocarboxylate transporter. *Biochem. Biophys. Res. Commun.* **217**:370–377 (1995).
18. J. Orlowski, R. A. Kandasamy, and G. E. Shull. Molecular cloning of putative members of the Na/H exchanger gene family. cDNA cloning, deduced amino acid sequence, and mRNA tissue expression of the rat Na/H exchanger NHE-1 and two structurally related proteins. *J. Biol. Chem.* **267**:9331–9339 (1992).
19. W. M. Pardridge. Brain Metabolism A perspective from the blood–brain barrier. *Physiol. Rev.* **63**:1481–1535 (1983).
20. S. E. Buchalter, M. R. Crain, and R. Kreisberg. Regulation of lactate metabolism in vivo. *Diabetes Metab. Rev.* **5**:379–391 (1989).
21. B. B. Brodie and C. A. M. Hogben. Some physico-chemical factors in drug action. *J. Pharm. Pharmacol.* **9**:345–380 (1957).
22. I. Tamai and A. Tsuji. Drug delivery through the blood-brain barrier. *Adv. Drug Deliv. Rev.* **19**:401–424 (1996).

23. C. K. Garcia, M. S. Brown, R. K. Pathak, and J. L. Goldstein. cDNA cloning of MCT2, a second monocarboxylate transporter expressed in different cells than MCT1. *J. Biol. Chem.* **270**:1843–1849 (1995).
24. M. Delvaux, M. J. Bastie, J. Chentoufi, E. J. Cragoe, N. Vaysse, and A. Ribet. Amiloride and analogues inhibit Na^+-H^+ exchange and cell proliferation in AR42J pancreatic cell line. *Am. J. Physiol.* **259**:G842–G849 (1990).
25. I. Tamai, H. Takanaga, H. Maeda, Y. Sai, T. Ogihara, H. Higashida, and A. Tsuji. Participation of a proton-cotransporter, MCT1, in the intestinal transport of monocarboxylic acids. *Biochem. Biophys. Res. Commun.* **214**:482–489 (1995).
26. A. J. Adler and R. E. Southwick. Distribution of glucose and lactate in the interphotoreceptor matrix. *Ophthalmic Res.* **24**:243–252 (1992).
27. E. Kenyon, A. Maminishkis, D. P. Joseph, and S. S. Miller. Apical and basolateral membrane mechanisms that regulate pH_i in bovine retinal pigment epithelium. *Am. J. Physiol.* **273**:C456–C472 (1997).
28. L. R. Drewes. Transport of the brain fuels, glucose and lactate. In O. B. Paulson, G. M. Knudsen, and T. Moos (eds.), *Brain Barrier Systems,* Munksgaard, Copenhagen, 1999, pp. 285–300.
29. G. M. Knudsen, O. B. Paulson, and M. M. Hertz. Kinetic analysis of the human blood-brain barrier transport of lactate and its influence by hypercapnia. *J. Cerebral. Blood Flow Metab.* **11**:581–586 (1991).